Laser sintering of coated polyamide 12: a new way to improve flammability

Marcos Batistella, Ouassila Kadri, Arnaud Regazzi, Monica Francesca Pucci, J. Lopez-Cuesta, Florence Ayme, David Bordeaux

Laser sintering of coated polyamide 12: a new way to improve flammability

Marcos Batistella[1,*], Ouassila Kadri[2], Arnaud Regazzi[3], Monica Francesca Pucci[3], José-Marie Lopez-Cuesta[1], Florence Ayme[2], and David Bordeaux[2]

[1] Polymers Composites and Hybrids (PCH), IMT Mines Ales, Ales, France
[2] SDTech, Ales, France
[3] LMGC, IMT Mines Ales, Univ Montpellier, CNRS, Ales, France

ABSTRACT

In this study coatings of kaolin and talc particles were successfully applied on the surface of polyamide 12 powder intended for laser sintering (LS). Microscopic observations revealed that using carboxymethyl cellulose (CMC) as surface modifier for fillers led to a better coverage of polymer grains with a surface coverage between 6 and 16% as a function of filler type and content. Differential scanning calorimetry measurements showed that the addition of talc and kaolin led to an increase in the crystallization temperature of PA12, but at the expense of processability. Process parameters were optimized in order to manufacture LS samples with the different coated powders. Fire behavior assessed by cone calorimetry showed that the use of CMC resulted in a significant decrease in the peak of heat release rate depending on the filler type and content. This behavior can be partially explained by an interaction between CMC, fillers and polymer, with the formation of amide linkage between carboxyl part of CMC and amine end groups of polyamide, resulting in an increase in the complex viscosity of materials.

Introduction

Various additive manufacturing (AM) techniques are available at industrial scale. Among them, laser sintering (LS) is attracting much attention because of its capability to build parts with very complex geometries without assembling. LS consists in the manufacturing of parts from CAD models using a layer-by-layer material deposition and consolidation approach. Powder layers, typically from 60 to 150 μm, are consecutively deposited and selectively fused often using a CO_2 laser beam. The process starts with the heating of the polymer powder to a temperature which is just below its melting point. A laser scans the powder bed and selectively melts the

Address correspondence to E-mail: marcos.batistella@mines-ales.fr

https://doi.org/10.1007/s10853-021-06621-7

polymer which corresponds to the layer of the object to be built. The build platform is lowered by the thickness of one layer, a new powder layer is applied, and the process repeats itself. The characteristics of LS allow its use for the production of prototypes or parts for various industries, as aerospace and defense, which have some of the toughest performance standards particularly in terms of flame retardancy. Moreover, the characteristics of LS process strongly limit the materials that can be used. In order to confer specific functional properties of parts made by LS, various studies evaluated the use of micronic or nanometric inorganic particles, such as, for example, glass beads [1], silicon carbide (SiC) [2], aluminum powders [3], hydroxyapatite (HA) [4], organo-modified clays [5] and silica [6]. Several studies focused on the incorporation of reinforcing materials to achieve mechanical properties enhancement of sintered parts made of polyamide 12 [7–9], whereas other studies evaluated the thermal and electrical properties using multi walled carbon nanotubes [10]. A series of works conducted by Ippolito et al. evaluated the influence of calcium carbonate on thermal properties of polyamide 12 prepared by extrusion [11–14]. In their work, the influence of particle size on crystallization and melting temperature was also evaluated. It was shown that, with a careful selection of particle size distribution, it is possible to tailor the crystallization kinetics of PA12 in order to enhance its processability by LS. However, some drawbacks of the use of fillers or reinforcements are their dispersion, changes in viscosity and interactions with the laser beam. Various methodologies were proposed in order to disperse particles in PA12 for LS process as grinding [15, 16], mechanical dry blending [17, 18] or solution mixing [6, 19]. Tan et al. [20] reported the advantages and disadvantages of the various composite powder preparation methods as well as their applications. The mechanical dry blending seems the simplest and the most common methodology to blend polymer powder and additives, fillers or reinforcements. However, the interaction and the surface coverage of polymer powder should be controlled in order to achieve a good melting and coalescence of particles. For example, Espera Jr. et al. [17] evaluated the addition of carbon black (1.5–10 wt%) by mechanical blending but showed that the addition of more than 3 wt% (which corresponds to a coverage of 4.26% of the surface of PA12 particles) appears detrimental to the mechanical properties.

Hence, a necessary condition to maximize the functionalities of submicronic particles such as carbon nanofillers of nanoclays is to perform a good dispersion in or on the polymer powder particles. The use of surfactants could be of prime interest to fulfil these objectives. Yuan et al. [21] used MWCNTs treated with a surfactant to ensure a good dispersion on PA12 powder particles. This method of surface coating in which polymer powders and nanofillers are dispersed using a water/surfactant solution to form a suspension was also applied to other polymer powders such as PEEK or TPU [22, 23]. Moreover, this method was also extended to phyllosilicates such as montmorillonite [5]. It is well known that various types of ultrafine of nanometric layered silicates are usually incorporated in polyamides to improve their properties. Kaolinite and talc can be processed at industrial scale in order to lead to ultrafine particles conferring similar reinforcement or barrier properties as organo-modified montmorillonites. Kaolin is an aluminosilicate with a theoretical formula of $Al_2Si_2O_5(OH)_4$. It is composed of one tetrahedral layer of silica (SiO4) linked to one octahedral sheet of alumina (AlO6) [24]. Talc is a magnesium silicate with a theoretical formula of $Mg_3Si_4O_{10}(OH)_2$ [25]. Various works in literature evaluated the influence of kaolin and talc in polypropylene [26, 27], ethylene vinyl acetate [28], polyamide 6 and 6,6 in terms of mechanical properties [29] and fire behavior [30, 31]. The incorporation of ultrafine particles of kaolin and talc lead to a noticeable improvement in terms of fire behavior due to their mode of action which is related to the formation of a protective surface layer. This mode of action was reported in the literature for various submicronic lamellar fillers [31–37] even though if their use is recommended in combination with usual flame retardants to achieve synergistic effects [38]. Nevertheless, some silicates have a negative influence on the polyamide degradation due to the release of water and the presence of hydroxyl surface groups which can induce the hydrolysis of macromolecular chains, impairing the thermal stability and processability of polymers. Some surface treatments such as silane coupling agents [31, 39–41] can interact with hydroxyl groups to prevent hydrolysis phenomena. They are also devoted to improve the dispersion and could change the viscoelastic behavior of composites which may lead to

an improved fire behavior [31]. Hence, it could be expected that some surface treatments carried out on ultrafine silicates through a surface coating method could be compatible with the LS process, promote dispersion and limit the hydrolysis of polyamide 12 powders processed by LS.

A previous study of our research group [18] evaluated the influence of various flame retardants and some layered silicates on the flowability and processability of PA12. It was shown that not all flame retardants commonly used for PA12 can be used in the production of LS parts. Considering that there is a lack of knowledge in literature regarding the fire behavior of polymers parts fabricated by LS and particularly regarding the influence of ultrafine layered silicates on the fire reaction of PA12, we propose to perform the surface coating of submicronic kaolin and talc particles on PA12 particles using carboxymethyl cellulose (CMC) as surfactant, applied through a fluidized bed. LS process parameters for such composites were designed in order to obtain standardized specimens allowing fire testing using cone calorimeter. The influence of the nature of the fillers and surface treatment on the flame retardant mechanisms were investigated.

Experimental

Materials

The commercial polyamide 12 powder used in this study (PA2200, EOS GmbH, Germany) has a mean diameter of 58 μm. The kaolinite (Paralux, Imerys) has a mean diameter of 0.8 μm and a specific surface area of 14.2 $m^2\ g^{-1}$. This grade of kaolinite is purified and contains only traces of TiO_2 and SiO_2. High aspect ratio talc (HAR T84, Imerys) has a mean diameter of 4.7 μm and a specific surface area of 19.5 $m^2\ g^{-1}$. This talc contains less than 20% of chlorite and 1–2% of dolomite. Sodium carboxymethylcellulose salt, with a molecular weight of 300–400 kDa, was supplied by Sigma.

Preparation

Coatings of fillers onto the PA2200 surface at 4 and 8 wt% were conducted in a fluidized bed equipment (Procell Labsystem, Glatt® GmbH, Germany) at 75 °C and an air flux of 75 $m^3\ h^{-1}$. A water solution containing 0.3% (w/w) of CMC was prepared and the desired amount of talc or kaolin was added to obtain solutions of 20% (w/w) for kaolin and 10% (w/w) for talc. This solution was injected into the fluidized bed equipment at a rate of 10 g min^{-1} to obtain the desired amount of kaolin or talc coated onto the PA surface. In order to evaluate the effect of the coating process and the presence of CMC, single polymer/fillers blends were carried out using a rotary drum mixer (Powder Mixing Station, EOS GmbH, Germany) at the same filler contents (i.e,. 4 and 8 wt%), using a rotation speed of 60 rpm for 15 min. Two square specimens of 70 × 70 × 4 mm^3 for cone calorimeter tests and six disks of 25 mm in diameter and 1 mm in thickness for rheological measurements were made by LS using a SnowWhite equipment from Sharebot (Italy). This printer has a build volume of 1.3 l and is equipped with a CO_2 laser. In all tests, the layer thickness and hatching distance were kept constant at 0.1 mm. Laser power and scan speed are discussed in "Thermal behavior and processability of composites". In order to evaluate the effect of processing on the rheological behavior, disks were also prepared by compression at 80 °C and a pressure of 20 bar.

Characterizations

The microstructure of powders and LS samples was analyzed using an environmental scanning electronic microscope (SEM) (Quanta 200 FEG, FEI Company, USA). Fourier-transform infrared spectroscopy (Vertex 70, Bruker) was conducted using an attenuated total reflectance module from 4000 to 400 cm^{-1} with a resolution of 1 cm^{-1}. Thermogravimetric analyses (SETSYS Evolution, Setaram Instrumentation, France) were conducted from 50 to 750 °C at 10 °C min^{-1} under a nitrogen flow of 100 mL min^{-1}. Samples of 10 ± 2 mg were used for differential scanning calorimetry (Diamond DSC, Perkin-Elmer, USA). A temperature ramp of 10 °C min^{-1} was applied to investigate the fusion and crystallization phenomena which define the SLS processing window. All tests were carried out on the powder mixtures, and first heating and cooling cycles were analyzed. Two tests were conducted for each formulation and means values are reported. Cone calorimeter experiments (Fire Testing Technology, UK) were carried out with an irradiance of 35 kW m^{-2} according to the ISO 5660 standard. For each formulation two plates were

tested. Surface specific area measurements of kaolin, talc and polyamide 12 were carried out with the BET method (TriStar II Plus, Micromeritics Instrument Corporation, USA).

Melt rheological properties were assessed with a rotational rheometer (MCR 702, Anton Paar, Austria) at 210 °C in a nitrogen atmosphere with a plate-plate geometry. Oscillatory dynamic measurements were performed at a constant strain of 5%. The frequency test range was carried out between 10^{-3} and 10^{2} rad s^{-1}. The tests were carried out in triplicate, and samples were dried at 80 °C in vacuum for 24 h to prevent hydrolysis of PA12.

Results and discussion

The nomenclature used hereafter to identify the materials is the following: KA and TA, respectively, for kaolin and talc, followed by their weight content (i.e., 4 or 8 wt%). The suffix CM identifies the formulations where CMC was used for coating.

Morphology characterization

In order to evaluate the effect of CMC in the PA12 powder coating, SEM observations were conducted on all formulations. Figures 1 and 2 show the microstructure of PA12 powders coated with kaolin and talc, respectively. Subfigures A and B show the microstructure of CMC coated clays at 4 and 8 wt%, respectively. These images show that the round shape of PA12 is maintained after the coating by kaolin or talc. However, some heterogeneities as a function of filler loading can be observed. For KACM4 formulation, it seems that the mineral particles cover the surface of the polymer powder and are oriented in a plate like direction. For the higher clay content (i.e., 8 wt%), some PA12 particles are completely coated while others are not, indicating some heterogeneities in these formulations.

The surface coverage of PA12 powder plays an important role in the efficiency of the LS process because it affects the adhesion between polymer particles as well as the melt viscosity. Assuming that kaolin and talc particles have a plate-like shape, it is possible to evaluate the surface coverage of PA12 powders by measuring the specific surface area of particles. BET measurements showed a specific surface of 4.5, 14.2 and 19.5 m^2 g^{-1} for PA12, kaolin and talc, respectively. Some results from literature show that, in the case of kaolin, edges contribute no more than 14% of the total surface area and each basal plane to 43% [42]. Assuming that each basal surface of kaolin and talc varies between 40 and 45% of the total particle surface, and that the filler particles are oriented in a plate like direction (as showed in SEM observations), it is possible to evaluate the surface coverage of PA12 powder by kaolinite and talc. It varies from 5.26 to 5.96% for KACM4 to 10.98–12.35% for KACM8 formulations, and from 7.22 to 8.13% for TACM4 to 15.07–16.96% for TACM8. Despite the relative low coverage of PA12 powder by fillers, especially for the lower contents, these values for talc and kaolin are higher than the optimum coverage found in the study of Espera et al. [17]. Furthermore,

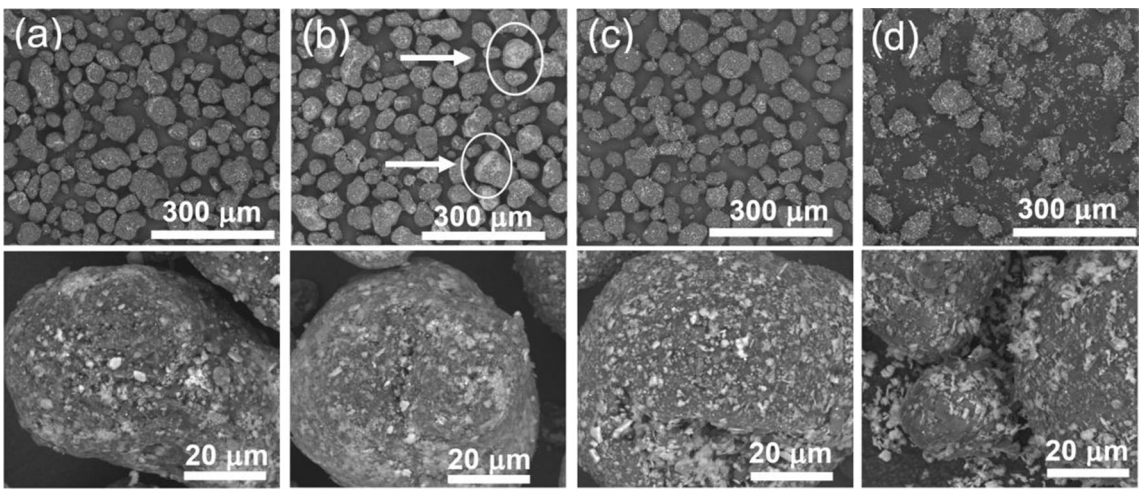

Figure 1 SEM images of kaolin coated PA12 powder: **a** KACM4; **b** KACM8; **c** KA4 and **d** KA8.

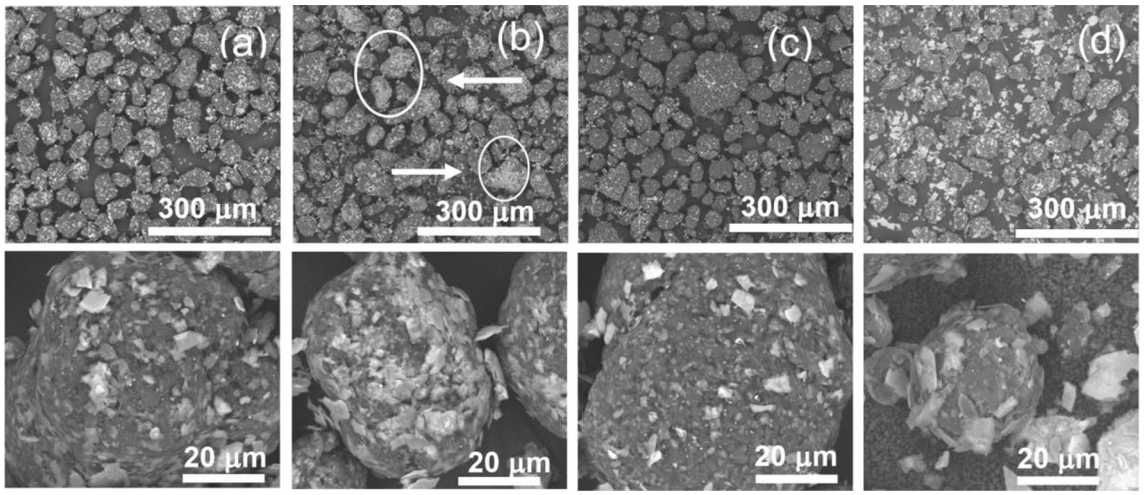

Figure 2 SEM images of talc coated PA12 powder: **a** TACM4; **b** TACM8; **c** TA4 and **d** TA8.

the formulations without CMC are expected to have a lower PA12 surface coverage due to a lower interaction between fillers and PA12 particles. However, the effect of coating on thermal behavior, especially on melting and crystallization temperatures should be considered in order to evaluate the processability of the formulations.

Thermal behavior and processability of composites

Thermograms of differential scanning calorimetry (DSC) are shown in Fig. 3 and characteristic temperatures are given in Table 1.

Due to the formation of γ crystalline structure of PA12 powders and to the high perfection of crystals, it has a sharp melting peak. The addition of kaolinite or talc resulted in a relative smoothing of melting peaks with a small increase in the onset melting temperature. This effect can be explained by the restriction of the macromolecular chains due to kaolin and talc.

The crystallization behavior changed as a function of the filler. For formulations containing kaolin, a relatively sharp crystallization peak was observed compared to neat PA12. This behavior can be explained by the presence of mineral particles that act as a nucleating agent and accelerate the crystallization process. For the formulations containing talc, it is possible to observe a broadening of the crystallization peak as well as an increase in the onset crystallization temperature. This behavior can be attributed to the higher amount of nucleation sites of talc particles, which has a higher specific surface than kaolin, that are more homogeneously distributed during cooling. This behavior was also reported by Ippolito et al. for calcium carbonate particles with controlled particle

Figure 3 DSC thermograms of formulations.

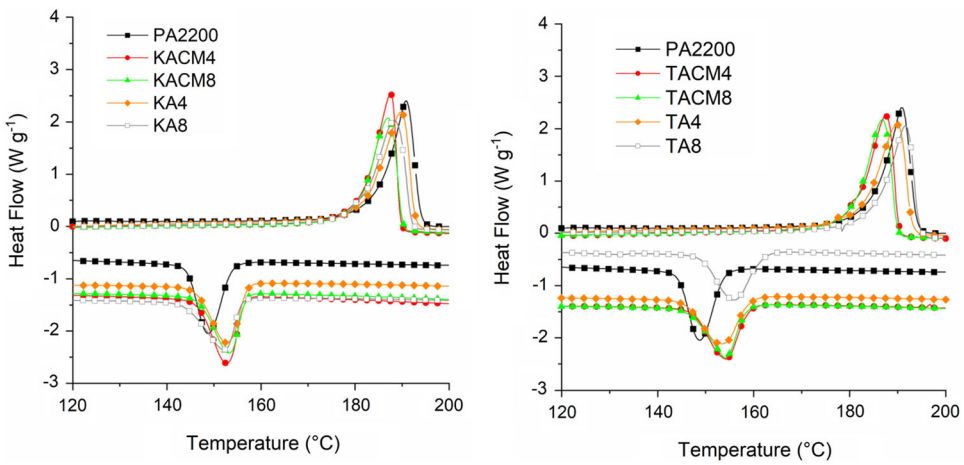

Table 1 DSC results of PA12 formulations

Sample	T_c Onset (°C)	T_m Onset (°C)	ΔT	T_c Peak (°C)	T_m Peak (°C)
PA2200	153	179	26	149	190
KACM4	156	181	25	153	188
KACM8	157	180	23	156	187
KA4	154	180	26	153	190
KA8	157	182	25	152	189
TACM4	157	180	23	154	187
TACM8	157	182	25	154	187
TA4	156	181	25	153	190
TA8	161	185	24	155	191

size distribution [14]. In this case, depending on the particle size and surface area, the amount of nucleation points increases, with an important impact on crystallization of PA12.

The changes in process parameters for composites compared to neat PA12 are always challenging because they imply changes in heat transfer, melt flow and laser-matter interaction. Yet, in order to evaluate the influence of fillers in terms of fire behavior, similar conditions were used for all formulations containing fillers, which are different from neat PA12, as shown in Table 2. These parameters were previously determined and were chosen as the parameters which lead to a success build and a lower porosity.

$$E_d = {}^{P_{LS}}/_{(V_{LS} \times d_{LS})} \quad (1)$$

It can be observed that, for processing formulations containing fillers, a lower density energy (E_d) and higher build chamber temperatures were used in order to build parts successfully. E_d was calculated as showed in Eq. (1) where P_{LS} is the laser power, V_{LS} is the laser scanning speed and d_{LS} is the hatching distance. The increase in build chamber temperature was necessary to avoid the curling of the parts. This is in agreement with results from DSC measurements where an increase in crystallization temperature was observed as a function of the filler type and content. Furthermore, various factors as crystallization speed and the time between layers could strongly limit the processing. Several authors described the dependence of the final part density to the relationship between temperature, energy density and duration between layers [43–45]. If the addition of a mineral particle increases the crystallization temperature, the risk of curling due to the rapid crystallization increases. However, if the bed temperature should be increased, the risk of polymer degradation may appear which could lead to a build failure. In the present study, a combination of high temperature and lower energy density was used to obtain parts successfully by LS. It is interesting to note that the addition of CMC did not lead to a significant difference in terms of processing temperature. Furthermore, the use of CMC had an important impact on powder flowability (Supplementary Information S1).

Table 2 Process parameters used for each formulation

Sample	Build chamber temperature (°C)	Laser power (W)	Laser scan speed (mm s^{-1})	Energy density (J cm^{-2})
PA2200	142	4.2	2700	1.6
KACM4	157	2.8	3600	0.8
KACM8	158	2.8	3600	0.8
KA4	160	2.8	3600	0.8
KA8	160	2.8	3600	0.8
TACM4	157	2.8	3000	0.9
TACM8	157	2.8	3000	0.9
TA4	158	2.8	2700	0.9
TA8	160	2.8	3000	0.9

For example, the addition of 8 wt% of talc leads to a powder bed presenting some heterogeneities (Fig S1 (a)), whereas the use of CMC leads to a homogeneous powder bed (Fig S1 (b)).

The microstructure of cryofractured LS samples is shown in Figs. 4 and 5. For all kaolin formulations (Fig. 4), low porosities were observed. When using CMC, the kaolinite particles seem to be still located at the boundaries of PA12 grains (arrows in Fig. 4a and b). It seems that, even though kaolin particles partially cover the surface of PA12, it has little effect on the melting and coalescence of PA12. On the contrary, the coverage of PA12 by untreated formulations (KA4 and KA8) was not observed, kaolinite particles being well dispersed in the matrix (Fig. 4c and d).

For formulations containing talc, a different behavior was observed. For TACM4 formulation (Fig. 5a), some polymer particles are not completely melted but it seems that talc particles are well dispersed in the matrix. The influence of talc regarding powder coalescence is more pronounced while increasing the talc content: in TACM8 (Fig. 5b), polymer particles are visible and partially melted. On the opposite, for the untreated formulations, polymer grains are almost completely melted (Fig. 5c and d). This behavior could be partially explained by the higher surface coverage of PA12 by talc particles compared to kaolin that could prevent the heat transfer and the melting of the polymer. Furthermore, talc could adsorb a higher amount of the laser radiation, preventing the melt and coalescence of PA12 powder.

Figure 6 shows mass loss curves of composites as a function of temperature. Two samples were tested for each formulation, and mean values are reported in Table 3. The initial thermal decomposition temperatures of the powders for 5, 20 and 50% weight loss are listed in Table 3.

Thermal degradation of PA12 starts at about 400 °C and occurs in two steps. The first is related to the main degradation of polyamides [46], and the second step corresponds to the degradation of the charred structure with no residue at 750 °C. The addition of CMC modified kaolinite or unmodified talc (TA8) led to an increase in $T_{5\%}$ and a decrease in the main degradation temperature ($T_{50\%}$). However, the addition of untreated kaolinite and CMC modified talc did not result in a significant difference in in $T_{5\%}$ and $T_{20\%}$ compared to neat polymer. It should be observed that the residue at 750 °C corresponds to around 75% of the content of each filler. The CMC

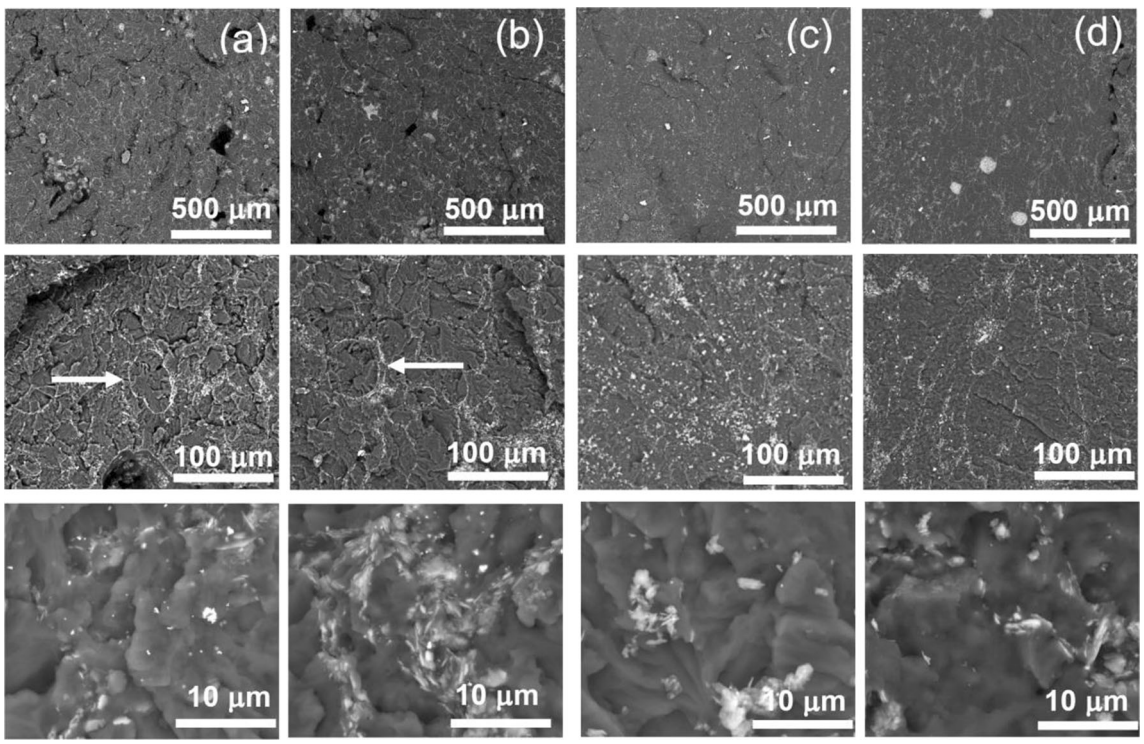

Figure 4 SEM images of SLS samples **a** KACM4; **b** KACM8; **c** KA4 and **d** KA8.

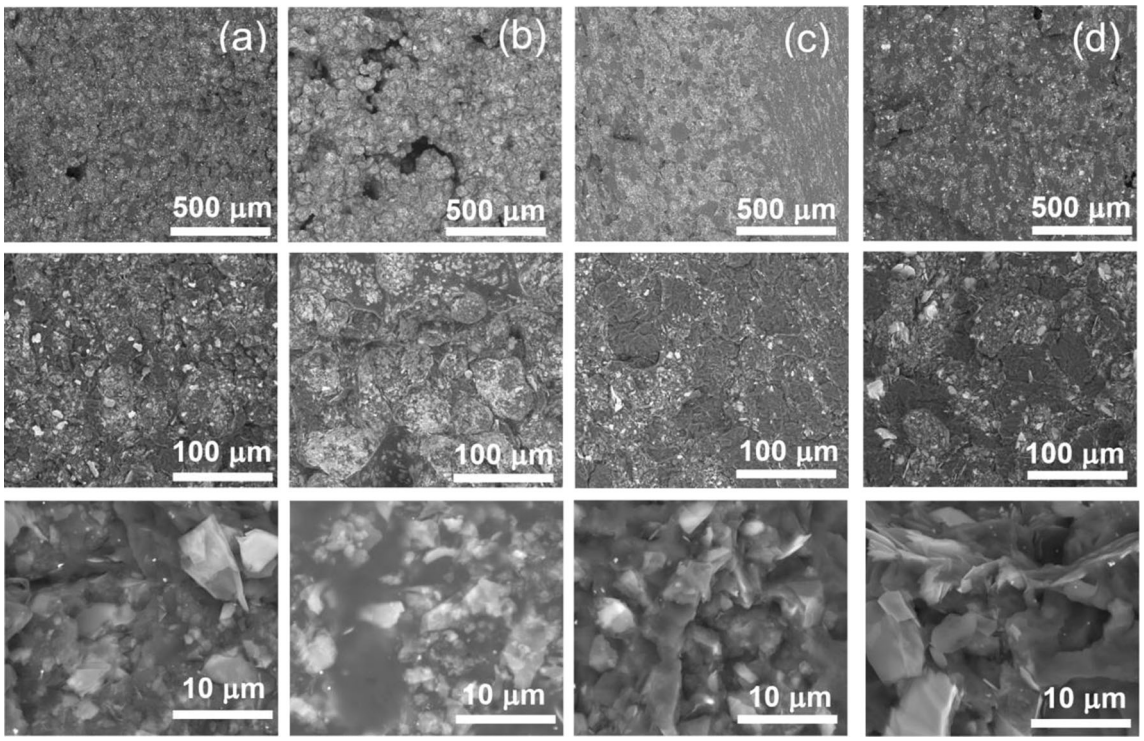

Figure 5 SEM images of SLS samples: **a** TACM4; **b** TACM8; **c** TA4 and **d** TA8.

Figure 6 TGA curves of composites under nitrogen at 10 °C min^{-1}.

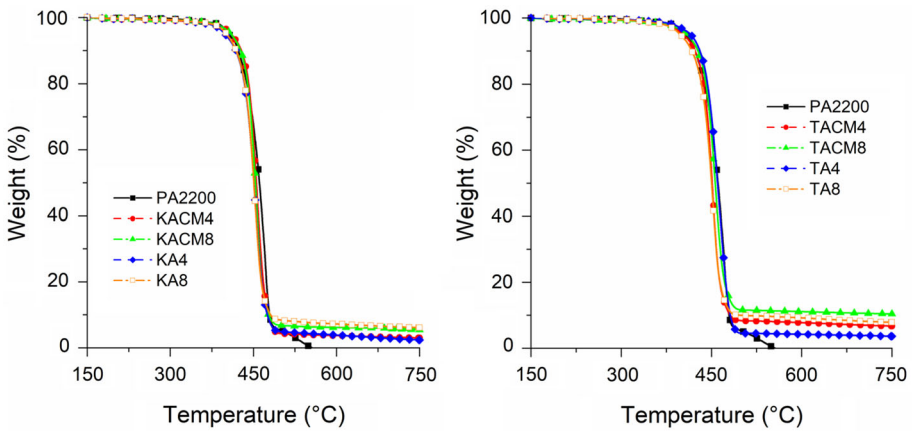

Table 3 Characteristic degradation temperatures under nitrogen at 10 °C min^{-1}

Sample	$T_{5\%}$ (°C)	$T_{20\%}$ (°C)	$T_{50\%}$ (°C)	Residue at 750 °C (%)
PA2200	405	438	461	0
KACM4	410	441	455	3
KACM8	409	440	454	6
KA4	398	434	451	3
KA8	402	434	451	6.2
TACM4	402	437	452	6.7
TACM8	408	441	456	10.3
TA4	415	443	460	3.6
TA8	399	435	450	6.2

modified talc compositions behaved differently since their residue was higher than the initial content, which could indicate a charring phenomenon conferred by the filler during the polymer degradation.

Cone calorimeter tests

Heat release rate (HRR) curves from cone calorimeter tests are shown in Fig. 7, while mean results (over two tests for each formulation) are presented in Table 4. Incorporation of both fillers allowed to improve the flame retardancy of the parts made by LS. This is illustrated by a reduction in the peak of heat release rate (pHRR) as a function of the filler type and content (Fig. 7).

The addition of untreated kaolin or talc led to a small reduction in pHRR and time to ignition (TTI) compared to neat polymer. The reduction in pHRR could be explained by the formation of a protective layer onto the surface of the sample. The reduction in TTI can be explained by the presence of hydroxyl groups which could catalyze PA12 degradation at lower temperatures.

The addition of CMC modified kaolin and talc led to a significant improvement in fire behavior with a greater decrease in the pHRR for the formulations containing 8 wt% of kaolin, and 4 and 8 wt% of talc compared to neat polymer and formulations containing unmodified fillers. It is interesting to note that an increase in the talc content (from 4 to 8 wt%) resulted in a small decrease in pHRR but to a higher decrease in TTI. Various factors could influence the TTI. In the case of additively manufactured samples, the porosity could play an important role [47] by trapping the volatile compounds and releasing them more quickly which could explain the observed reduction in TTI of the TACM8 samples.

Small differences were observed in total heat release (THR) and effective heat of combustion (EHC) values, indicating that the predominant mode of action is the formation of a protective surface layer and an increase in viscosity, which could reduce the rate of volatile gases released [26, 48]. An increase in total smoke release (TSR) was observed for all samples except for KACM4. However, the addition of CMC resulted in a decrease in TSR compared to samples without CMC. The presence of hydroxyl sites on the surface of the fillers could lead to changes in the degradation pathway of the polymers by the production of higher amount of CO (see supporting information S2).

In all cases, it should be noted that residues at the end of the test were slightly higher than the filler content. This result was the most pronounced for the talc compositions with CMC.

Rheological measurements

Literature results show that surface treatments of fillers could entail different effects. In particular, improvements of the dispersion may have an important impact on mechanical properties and fire behavior [26, 48]. The surface treatment of fillers could lead to an increase in viscosity due to the increase in dispersion as well as some chemical interaction with polymer chains. This increase in viscosity could reduce the transfer of degradation products from condensed to gas phase, which could result in a decrease in pHRR.

Moreover, depending on the nature of the filler, it could act as a lubricating agent with a decrease in

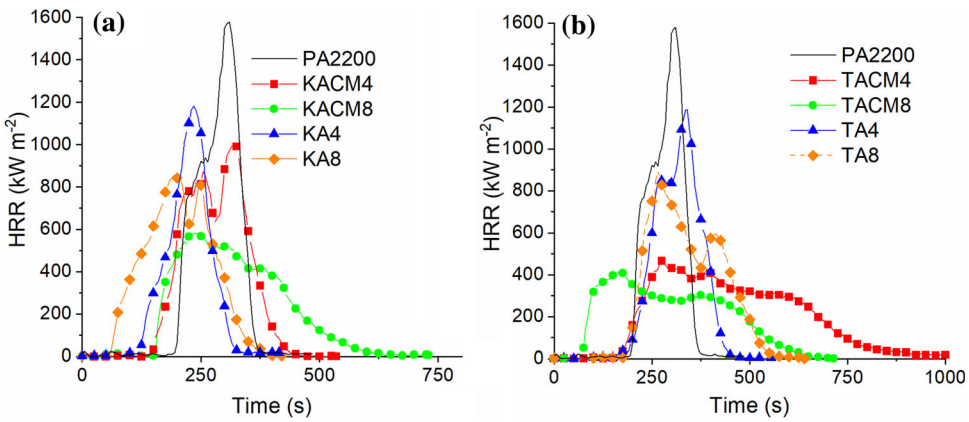

Figure 7 Cone calorimeter results of formulations **a** kaolin and **b** talc.

Table 4 Cone calorimeter results of formulations containing coated and uncoated kaolin and talc

Sample	TTI (s)	pHRR (kW m^{-2})	EHC (kJ g^{-1})	THR (MJ m^{-2})	TSR (m^2 m^{-2})	Residue (%)
PA2200	197	1580	34	151	1723	–
KACM4	137	1090	35	152	1459	8.5
KACM8	145	673	32	159	1847	8.7
KA4	132	1060	33	152	1942	6
KA8	55	854	29	148	2050	9
TACM4	110	528	38	157	1870	8
TACM8	88	502	37	155	1907	12
TA4	172	1162	37	151	1949	6
TA8	180	890	38	149	2030	10

viscosity. In order to evaluate the influence of CMC surface treatment onto PA12 composites, viscosity measurements were conducted on LS samples. The corresponding complex viscosity (η*) curves are presented in Fig. 8.

From Fig. 8, it can be seen that the viscosity of all samples decreased with an increase in frequency, indicating a shear thinning behavior. Furthermore, compared to neat PA12, the viscosity of composites was raised significantly except for KA4 formulation. It can be observed that the addition of 4 wt% of unmodified kaolin resulted in a decrease in complex viscosity at lower frequencies and in a slightly increase at higher frequencies compared to neat PA12. A percentage of 8 wt% of kaolin resulted in an increase in complex viscosity compared to neat polymer and to KA4. The surface modification of CMC led to a further rise compared to untreated formulations. The addition of talc also resulted in higher values of complex viscosity at higher frequencies for all formulations compared to PA12. At lower frequency, all formulations showed the same behavior, with viscosity values close to those of neat PA12. Some results found in literature suggest that the surface modification of particles could increase the viscosity if chemical bonding occurs [49, 50]. However, some interfacial agents could act only as a wetting agents [49] which could explain the lower increase in complex viscosity of formulations containing talc.

Viscosity has also a high impact on LS parts with an increase in part porosity if the viscosity is too high, especially at low frequencies. Comparing the viscosity values of talc formulations at low frequencies, little difference was observed compared to neat PA12. This indicates that the composites require a similar duration as to neat PA12 to fuse and coalesce. However, lower melt and coalescence were observed for these formulations (Fig. 5). This behavior suggests that talc particles absorbed and/or reflected a

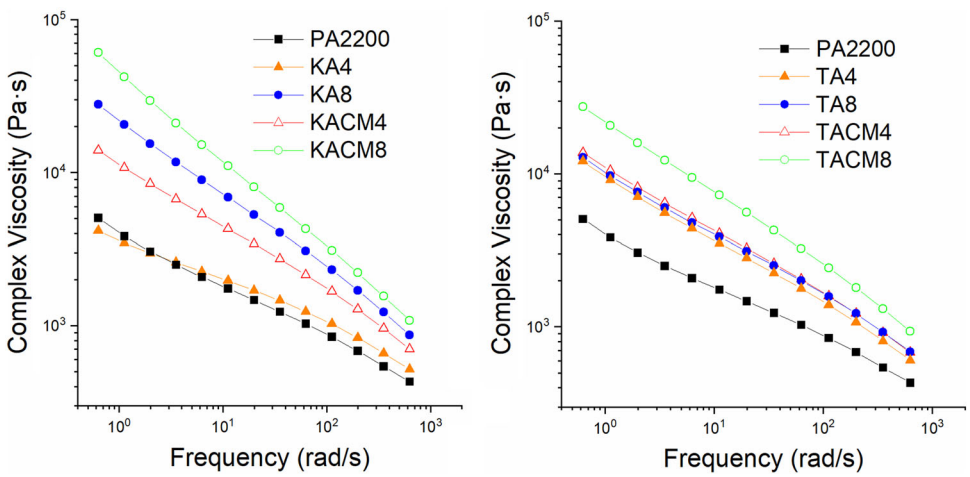

Figure 8 Complex viscosities of LS samples at 210 °C as a function of frequency.

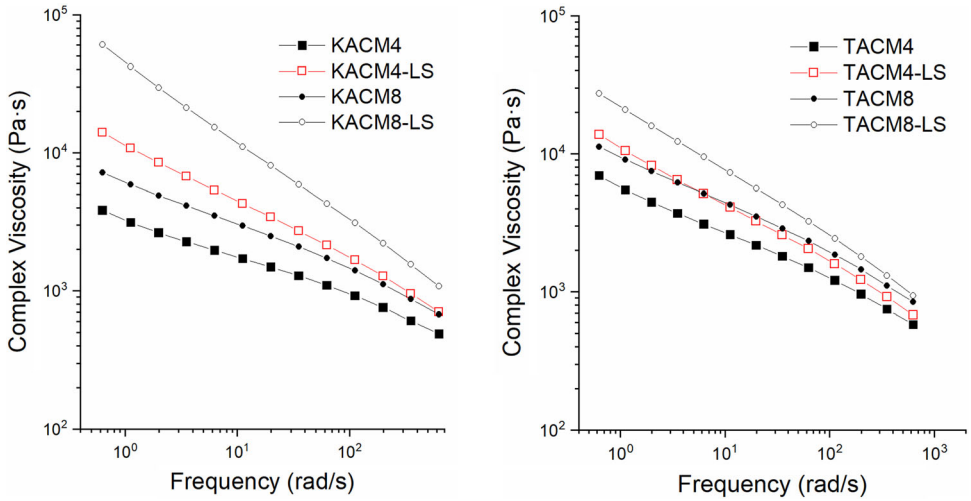

Figure 9 Complex viscosities of CMC formulations at 210 °C prepared by LS and compression molding.

significant energy from the laser, preventing the complete coalescence of polymer grains.

Compared to the PA12 samples, filled PA12- showed an increase in storage (G') and loss (G'') moduli (Supporting Information, Figs. S2 and S3), except for KA4 and KACM4 formulations. With the increase in talc and kaolin loading, G' and G'' were also increased slightly, with higher valuer for KACM8. It is interesting to note that the surface modification of kaolin leads to a decrease in G' and G'' but for talc a slight increase is observed. Furthermore, an increased G' means a more elastic structure, which indicates the limitation of polymer chain motion due to the fillers and may partially explain the higher porosity of samples containing talc.

Comparing rheological measurements conducted on pressed and LS samples (Fig. 10), it is possible to observe an increase in complex viscosity for LS samples, indicating some interaction between components due to processing. This behavior can be explained by the formation of amide linkages between carboxyl groups of CMC and end amine groups of polyamide, which are formed at temperatures higher than 250 °C. Such temperatures can be achieved during LS, at least locally for a short

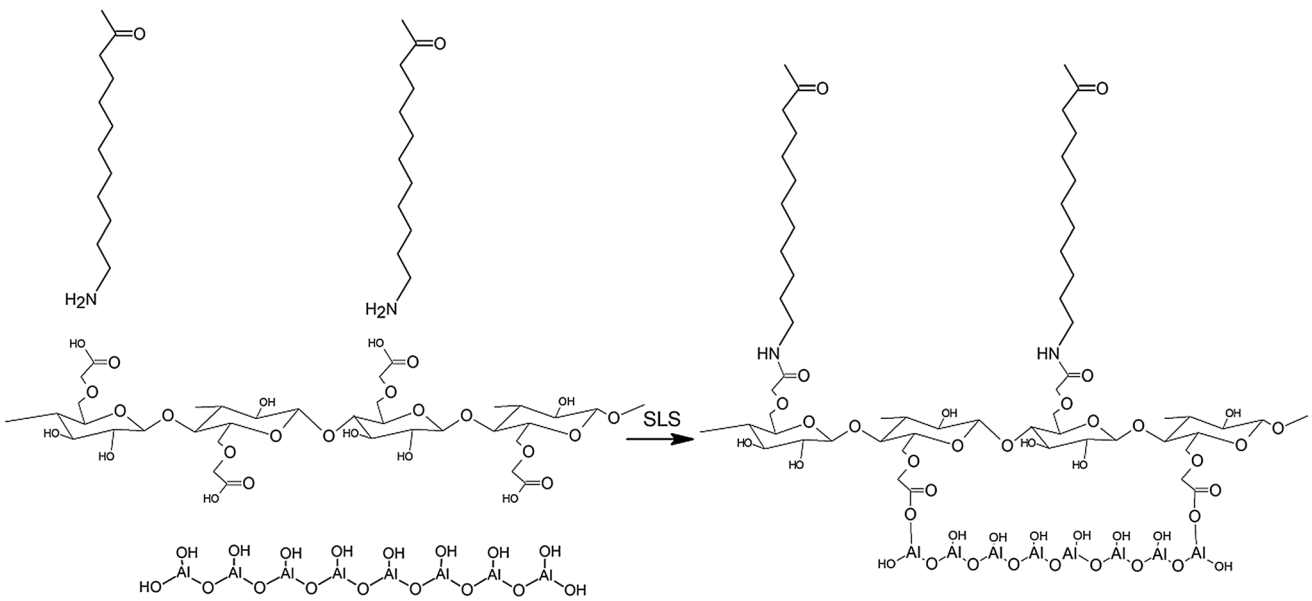

Figure 10 Schematic amide linkage between carboxylic group of carboxymethylcellulose and amine end groups of polyamide.

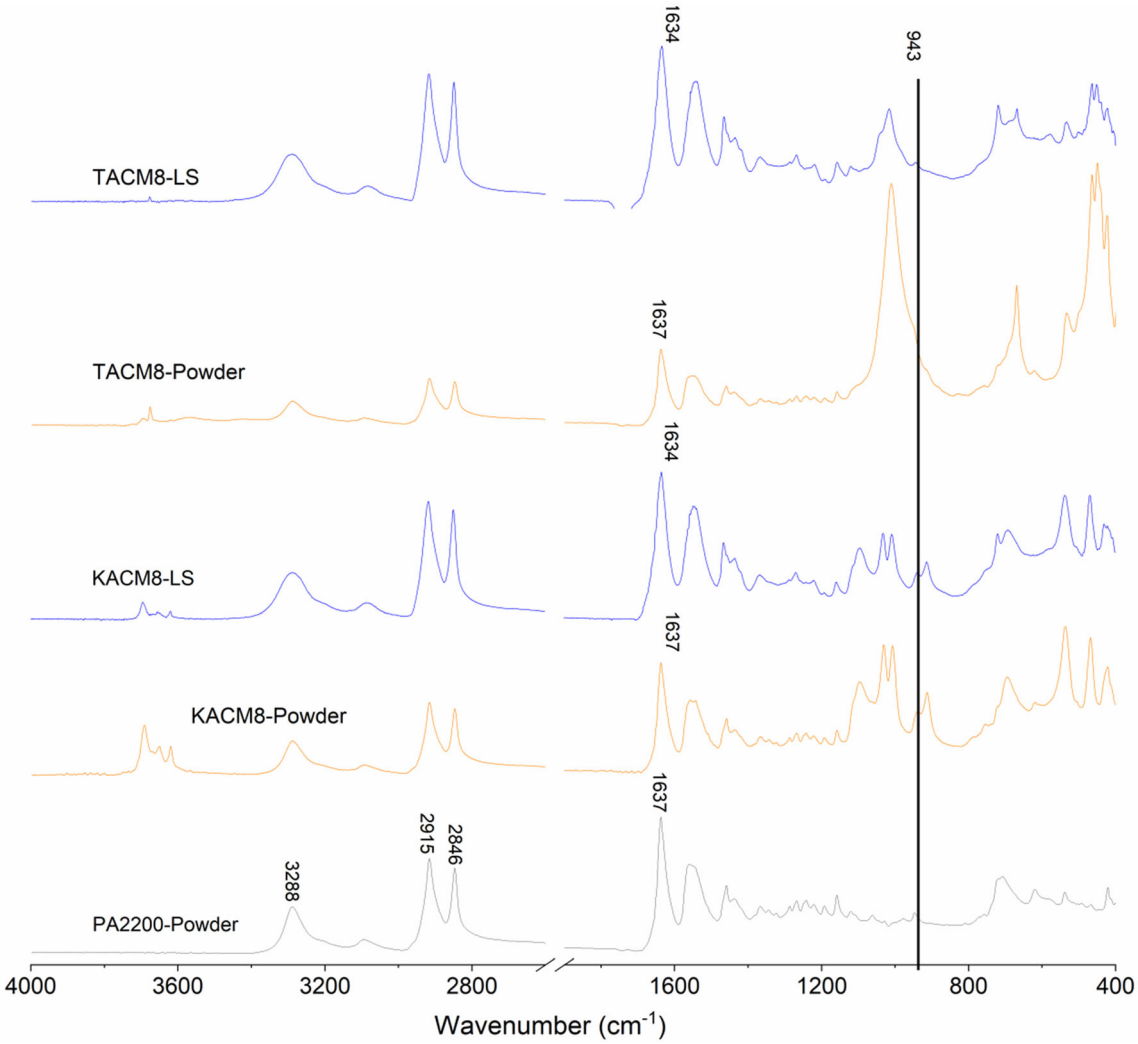

Figure 11 FTIR results of KACM8 and TACM8 materials before (powder) and after (SLS) manufacturing.

duration [51]. Carboxylic groups can also react with hydroxyl groups present at the surface of clays, leading to the formation of hydrogen bonds, which can contribute to the increase observed in viscosity. It was shown that the carboxyl groups of CMC could react with the magnesium sites onto the surface of the talc by a bidentate chelating bond [52]. The formation of amide linkages could result in an increase in complex viscosity due to a restriction of polymer chain motion. This increase in complex viscosity can also partially explain the improved fire behavior of CMC treated samples.

In order to evaluate the interaction between CMC and PA12, FTIR measurements were conducted on KACM8 and TACM8 powders and compared to the same formulations made by LS.

FTIR results (Fig. 11) show the characteristic vibrations of PA12, talc and kaolin. The spectrogram shows the absorption bands at 3288 and 1555 cm^{-1} which correspond to the stretching and bending vibrations of the N–H group. The absorption at 1637 cm^{-1} and 1542 cm^{-1} can be assigned to the amide I and amide II bands [53, 54]. Besides vibration peaks of PA12, spectrogram of formulations containing kaolin show the characteristic vibration bands of kaolinite hydroxyl groups at 3687, 3650 and 3619 cm^{-1}. Talc formulations (TACM8-powder and TACM8-LS) show the stretching vibrational bands of Si–O–Si at 466 and 1010 cm^{-1} and the band at 669 cm^{-1} correspond the Si–O-Mg bond. The band at and 3675 cm^{-1} can be attributed to the vibrations of talc hydroxyl groups [55, 56].

The spectra of LS samples are slightly different compared to powders. The vibration band at 1637 cm^{-1}, which corresponds to the C=O and C–N bonds, decreases to 1634 cm^{-1} for both KACM8 and TACM8. This change could suggest the formation of hydrogen bonds between N–H groups of PA12 and C=O of CMC [57].

It also should be noted that kaolin and talc have adsorption bands at 943 cm^{-1} (which correspond to a wavelength of 10.6 μm) indicating that both fillers absorbs a part of the laser irradiation. As showed in Figs. 1 and 2, some PA12 particles are completely coated by fillers, whereas others are only partially coated. This behavior indicates that fillers should, at least partially, absorb the laser beam and then transfer heat to PA12 while keeping the round shape of polymer powder. This behavior can be observed in Fig. 4, where CMC modified kaolin particles seem to form circles around polymer particles, which completely melted. In this case, the role of CMC is to enhance the heat transfer by conduction [58], which correlates with the lower porosity found in the samples containing kaolin.

In the case of compositions containing CMC surface modified talc, it is shown in Fig. 5 that PA12 is not completely melted, indicating that talc could differently interact with laser beam or that the heat transfer from talc to PA12 is slower. Furthermore, talc particles have a higher aspect ratio than kaolin, leading to a higher surface coating of PA12. This implies that the time of direct irradiation of polymer is shorter than that of kaolin, which limits polymer melting before a new layer is applied, leading to a more porous part.

It should be noted that optical properties of talc are certainly different from PA12, leading to a different behavior. Tolocko et al. conducted some investigations of optical characteristics of different polymers used in LS using an integration sphere at a wavelengths of 1.06 and 10.6 μm [59, 60]. These authors showed that PA12 absorbs 85% of the laser energy at 10.6 μm and reflects 5% at this wavelength. In the case of talc, it could absorb/reflect in a different way than PA12 which could also explain the higher porosity observed in these samples.

Conclusions

Many factors can prevent a successful processing of particulate composites via LS. Most of them can be attributed to the differences of thermo-physical properties between polymer and mineral particle powders. Besides these properties, physico-chemical interactions between components induced by the laser irradiation as well as their initial location in the powder bed can influence the LS processability and the final properties of composites.

CMC was used for coating kaolin and talc onto PA12 through an original process of fluidized bed in order to maximize the coverage of the polymer powder by the mineral particles.

However, the higher surface coverage of PA12 by talc particles induced thermal changes, leading to limited melting and coalescence of the polymer as well as a significant porosity fraction. Due to the powder rheology and fillers/laser interaction changes, processing parameters were tuned in order to achieve a successful build.

Even though the surface coverage can play an important role in terms of printability, no difference in terms of processability was observed in the studied range for kaolin coated samples.

The surface treatment of fillers with CMC was able to improve the powder flowability as well as the fire behavior of composites. This can be ascribed to an interaction between CMC and polyamide with the formation of amide linkages, which increases the viscosity and limits the possible hydrolysis of polymer chains due to hydroxyl groups present at the surface of kaolin and, at lower extent on the surface of the talc.

Finally, the use of 8 wt% of talc with CMC was particularly interesting for reducing the heat release rate during combustion of PA12.

These results have shown that an accurate assessment of the processing parameters depends strongly on a good knowledge of the thermo-physical properties of the various components as well as their interactions with the laser beam. Further studies will be carried out to improve the understanding of these complex systems using model compositions.

Acknowledgements

The authors would like to thank the European Union (FEDER funding for the Occitanie region), the Occitanie region for funding the POLIFRIL project.

Funding

This study was funded by European Union (FEDER funding for the Occitanie region – POLIFRIL Project).

Declarations

Conflict of interest The authors declare that they have no conflict of interest.

Supplementary Information: The online version contains supplementary material available at https://doi.org/10.1007/s10853-021-06621-7.

References

[1] Cano AJ, Salazar A, Rodríguez J (2018) Effect of temperature on the fracture behavior of polyamide 12 and glass-filled polyamide 12 processed by selective laser sintering. Eng Fract Mech 203:66–80. https://doi.org/10.1016/j.engfracmech.2018.07.035

[2] Hon KKB, Gill TJ (2003) Selective laser sintering of SiC/polyamide composites. CIRP Ann Manuf Technol 52:173–176. https://doi.org/10.1016/S0007-8506(07)60558-7

[3] Mazzoli A, Moriconi G, Pauri MG (2007) Characterization of an aluminum-filled polyamide powder for applications in selective laser sintering. Mater Des 28:993–1000. https://doi.org/10.1016/j.matdes.2005.11.021

[4] Feng P, Niu M, Gao C, et al (2014) A novel two-step sintering for nano-hydroxyapatite scaffolds for bone tissue engineering. Sci Rep 4

[5] Tan LJ, Zhu W, Zhou K (2020) Development of organically modified montmorillonite/polypropylene composite powders for selective laser sintering. Powder Technol 369:25–37. https://doi.org/10.1016/j.powtec.2020.05.005

[6] Chunze Y, Yusheng S, Jinsong Y, Jinhui L (2009) A nanosilica/nylon-12 composite powder for selective laser sintering. J Reinf Plast Compos 28:2889–2902. https://doi.org/10.1177/0731684408094062

[7] Dadbakhsh S, Verbelen L, Vandeputte T et al (2016) Effect of powder size and shape on the SLS processability and mechanical properties of a TPU elastomer. Phys Procedia 83:971–980. https://doi.org/10.1016/j.phpro.2016.08.102

[8] Borille AV, De Oliveira GJ, Lopes D (2017) Geometrical analysis and tensile behaviour of parts manufactured with flame retardant polymers by additive manufacturing. Rapid Prototyp J 23:169–180. https://doi.org/10.1108/RPJ-09-2015-0130

[9] Majewski C, Zarringhalam H, Hopkinson N (2008) Effect of the degree of particle melt on mechanical properties in selective laser-sintered Nylon-12 parts. Proc Inst Mech Eng Part B J Eng Manuf 222:1055–1064. https://doi.org/10.1243/09544054JEM1122

[10] Yuan S, Zheng Y, Chua CK et al (2018) Electrical and thermal conductivities of MWCNT/polymer composites fabricated by selective laser sintering. Compos A Appl Sci Manuf 105:203–213. https://doi.org/10.1016/j.compositesa.2017.11.007

[11] Ippolito F, Hübner G, Claypole T, Gane P (2021) Calcium carbonate as functional filler in polyamide 12-manipulation of the thermal and mechanical properties. Processes 9. https://doi.org/10.3390/pr9060937

[12] Ippolito F, Hübner G, Claypole T, Gane P (2020) Influence of the surface modification of calcium carbonate on polyamide 12 composites. Polymers (Basel) 12. https://doi.org/10.3390/polym12061295

[13] Ippolito F, Hübner G, Claypole T, Gane P (2021) Impact of bimodal particle size distribution ratio of functional calcium carbonate filler on thermal and flowability properties of polyamide 12. Appl Sci 11:1–13. https://doi.org/10.3390/app11020641

[14] Ippolito F, Rentsch S, Hübner G et al (2019) Influence of calcium carbonate on polyamide 12 regarding melting, formability and crystallization properties. Compos Part B Eng 164:158–167. https://doi.org/10.1016/j.compositesb.2018.11.079

[15] Schmidt J, Sachs M, Fanselow S et al (2016) Optimized polybutylene terephthalate powders for selective laser beam melting. Chem Eng Sci 156:1–10. https://doi.org/10.1016/j.ces.2016.09.009

[16] Koo JH, Pilato L, Wissler G, et al (2005) Innovative selective laster sintering rapid manufacturing using nanotechnology. 16th Solid Free Fabr Symp SFF 2005 11:98–108

[17] Espera AH, Valino AD, Palaganas JO et al (2019) 3D printing of a robust polyamide-12-carbon black composite via selective laser sintering: thermal and electrical conductivity. Macromol Mater Eng 304:1–8. https://doi.org/10.1002/mame.201800718

[18] Batistella M, Regazzi A, Pucci MF et al (2020) Selective laser sintering of polyamide 12/flame retardant

compositions. Polym Degrad Stab 181:109318. https://doi.org/10.1016/j.polymdegradstab.2020.109318

[19] Zhu W, Yan C, Shi Y, et al (2016) A novel method based on selective laser sintering for preparing high-performance carbon fibres/polyamide12/epoxy ternary composites. Sci. Rep. 6

[20] Tan LJ, Zhu W, Zhou K (2020) Recent progress on polymer materials for additive manufacturing. Adv Funct Mater 30:1–54. https://doi.org/10.1002/adfm.202003062

[21] Yuan S, Bai J, Chua CK et al (2016) Highly enhanced thermal conductivity of thermoplastic nanocomposites with a low mass fraction of MWCNTs by a facilitated latex approach. Compos Part A Appl Sci Manuf 90:699–710. https://doi.org/10.1016/j.compositesa.2016.09.002

[22] Chen B, Berretta S, Evans K et al (2018) A primary study into graphene/polyether ether ketone (PEEK) nanocomposite for laser sintering. Appl Surf Sci 428:1018–1028. https://doi.org/10.1016/j.apsusc.2017.09.226

[23] Gan X, Wang J, Wang Z et al (2019) Simultaneous realization of conductive segregation network microstructure and minimal surface porous macrostructure by SLS 3D printing. Mater Des 178:107874. https://doi.org/10.1016/j.matdes.2019.107874

[24] Frost RL (1997) Kaolinite hydroxyls-a raman microscopy study. Clay Miner 32:471–484. https://doi.org/10.1180/claymin.1997.032.3.09

[25] Olabanji SO, Ige AO, Mazzoli C et al (2005) Quantitative elemental analysis of an industrial mineral talc, using accelerator-based analytical technique. Nucl Instruments Methods Phys Res Sect B Beam Interact with Mater Atoms 240:327–332. https://doi.org/10.1016/j.nimb.2005.06.159

[26] Batistella M, Otazaghine B, Sonnier R et al (2016) Fire retardancy of polypropylene/kaolinite composites. Polym Degrad Stab 129:260–267. https://doi.org/10.1016/j.polymdegradstab.2016.05.003

[27] Almeras X, Le Bras M, Hornsby P et al (2003) Effect of fillers on the fire retardancy of intumescent polypropylene compounds. Polym Degrad Stab 82:325–331. https://doi.org/10.1016/S0141-3910(03)00187-3

[28] Clerc L, Ferry L, Leroy E, Lopez-Cuesta J-MM (2005) Influence of talc physical properties on the fire retarding behaviour of (ethylene–vinyl acetate copolymer/magnesium hydroxide/talc) composites. Polym Degrad Stab 88:504–511. https://doi.org/10.1016/j.polymdegradstab.2004.12.010

[29] Ansari DM, Price GJ (2004) Correlation of mechanical properties of clay filled polyamide mouldings with chromatographically measured surface energies. Polymer (Guildf) 45:3663–3670. https://doi.org/10.1016/j.polymer.2004.03.045

[30] Batistella MA, Sonnier R, Otazaghine B et al (2018) Interactions between kaolinite and phosphinate-based flame retardant in Polyamide 6. Appl Clay Sci 157:248–256. https://doi.org/10.1016/j.clay.2018.02.021

[31] Batistella M, Caro-Bretelle ASS, Otazaghine B et al (2015) The influence of dispersion and distribution of ultrafine kaolinite in polyamide-6 on the mechanical properties and fire retardancy. Appl Clay Sci 116–117:8–15. https://doi.org/10.1016/j.clay.2015.07.034

[32] Qin H, Su Q, Zhang S et al (2003) Thermal stability and flammability of polyamide 66/montmorillonite nanocomposites. Polymer (Guildf) 44:7533–7538. https://doi.org/10.1016/j.polymer.2003.09.014

[33] Vahabi H, Batistella MAA, Otazaghine B et al (2012) Influence of a treated kaolinite on the thermal degradation and flame retardancy of poly(methyl methacrylate). Appl Clay Sci 70:58–66. https://doi.org/10.1016/j.clay.2012.09.013

[34] Marney DCO, Russell LJ, Wu DY et al (2008) The suitability of halloysite nanotubes as a fire retardant for nylon 6. Polym Degrad Stab 93:1971–1978

[35] Dahiya JBB, Muller-Hagedorn M, Bockhorn H, Kandola BKK (2008) Synthesis and thermal behaviour of polyamide 6/bentonite/ammonium polyphosphate composites. Polym Degrad Stab 93:2038–2041. https://doi.org/10.1016/j.polymdegradstab.2008.02.016

[36] Jang B, Wilkie C (2005) The effect of clay on the thermal degradation of polyamide 6 in polyamide 6/clay nanocomposites. Polymer (Guildf) 46:3264–3274. https://doi.org/10.1016/j.polymer.2005.02.078

[37] Lao SCC, Wu C, Moon TJJ et al (2009) Flame-retardant polyamide 11 and 12 nanocomposites: Thermal and flammability properties. J Compos Mater 43:1803–1818. https://doi.org/10.1177/0021998309338413

[38] Lopez-Cuesta J, Laoutid F (2009) Multicomponent FR Systems. In: Wilkie CA, Morgan AB (eds) Fire retardancy of polymeric materials, 2nd edn. CRC Press, Boca Raton, pp 301–328

[39] Domka L, Malickaa A, Stachowiakc N et al (2008) The effect of kaolin modification of silane coupling agents on the properties of the polyethylene composites. Polish J Chem Technol 10:5–10. https://doi.org/10.2478/v10026-008-0020-8

[40] Buggy M, Bradley G, Sullivan A (2005) Polymer–filler interactions in kaolin/nylon 6,6 composites containing a silane coupling agent. Compos A Appl Sci Manuf 36:437–442. https://doi.org/10.1016/j.compositesa.2004.10.002

[41] Domka L, Malicka A, Stachowiak N (2010) The effect of kaolin modification of silane coupling agents on the properties of the polyethylene composites, pp 5–10

[42] Brady PVP, Cygan RTR, Nagy KL (1996) Molecular controls on kaolinite surface charge. J Colloid Interface Sci 183:356–364

[43] Wegner A, Witt G (2015) Understanding the decisive thermal processes in laser sintering of polyamide 12. AIP Conf Proc 1664:1–6. https://doi.org/10.1063/1.4918511

[44] Drummer D, Wudy K, Drexler M (2014) Influence of energy input on degradation behavior of plastic components manufactured by selective laser melting. Phys Procedia 56:176–183. https://doi.org/10.1016/j.phpro.2014.08.160

[45] Drummer D, Drexler M, Wudy K (2015) Density of laser molten polymer parts as function of powder coating process during additive manufacturing. Procedia Eng 102:1908–1917. https://doi.org/10.1016/j.proeng.2015.01.331

[46] Mailhos-Lefievre V, Sallet D, Martel B et al (1989) Thermal degradation of pure and flame-retarded polyamides 11 and 12. Polym Degrad Stab 23:327–336. https://doi.org/10.1016/0141-3910(89)90055-4

[47] Regazzi A, Pucci MF, Dumazert L et al (2019) Controlling the distribution of fire retardants in poly(lactic acid) by fused filament fabrication in order to improve its fire behaviour. Polym Degrad Stab 163:143–150. https://doi.org/10.1016/j.polymdegradstab.2019.03.008

[48] Kashiwagi T, Mu M, Winey K et al (2008) Relation between the viscoelastic and flammability properties of polymer nanocomposites. Polymer (Guildf) 49:4358–4368. https://doi.org/10.1016/j.polymer.2008.07.054

[49] Bigg DM (1982) Rheological analysis of highly loaded polymeric composites filled with non-agglomerating spherical filler particles. Polym Eng Sci 22:512–518. https://doi.org/10.1002/pen.760220810

[50] Han CD, Van Den Weghe T, Shete P, Haw JR (1981) Effects of coupling agents on the rheological properties, processability, and mechanical properties of filled polypropylene. Polym Eng Sci 21:196–204. https://doi.org/10.1002/pen.760210404

[51] Bai J, Goodridge RD, Yuan S et al (2015) Thermal Influence of CNT on the polyamide 12 nanocomposite for selective laser sintering. Molecules 20:19041–19050. https://doi.org/10.3390/molecules201019041

[52] Cuba-Chiem LT, Huynh L, Ralston J, Beattie DA (2008) In situ particle film ATR-FTIR studies of CMC adsorption on talc: the effect of ionic strength and multivalent metal ions. Miner Eng 21:1013–1019. https://doi.org/10.1016/j.mineng.2008.03.007

[53] Roy S, Das T, Zhang L et al (2015) Triggering compatibility and dispersion by selective plasma functionalized carbon nanotubes to fabricate tough and enhanced Nylon 12 composites. Polymer (Guildf) 58:153–161. https://doi.org/10.1016/j.polymer.2014.12.032

[54] Rafiq R, Cai D, Jin J, Song M (2010) Increasing the toughness of nylon 12 by the incorporation of functionalized graphene. Carbon N Y 48:4309–4314. https://doi.org/10.1016/j.carbon.2010.07.043

[55] Marzbani P, Resalati H, Ghasemian A, Shakeri A (2016) Surface modification of talc particles with phthalimide: study of composite structure and consequences on physical, mechanical, and optical properties of deinked pulp. BioResources 11. https://doi.org/10.15376/biores.11.4.8720-8738

[56] Kloprogge JT, Frost RL, Rintoul L (1999) Single crystal Raman microscopic study of the asbestos mineral chrysotile. Phys Chem Chem Phys 1:2559–2564. https://doi.org/10.1039/a809238i

[57] Chowdhury R, Banerji MS, Shivakumar K (2006) Development of acrylonitrile-butadiene (NBR)/polyamide thermoplastic elastomeric compositions: effect of carboxylation in the NBR phase. J Appl Polym Sci 100:1008–1012. https://doi.org/10.1002/app.22876

[58] Gerstner P, Paltakari J, Gane PAC (2009) A lumped parameter model for thermal conductivity of paper coatings. Transp Porous Media 78:1–9. https://doi.org/10.1007/s11242-008-9276-y

[59] Tolochko NK, Khlopkov YV, Mozzharov SE et al (2000) Absorptance of powder materials suitable for laser sintering. Rapid Prototyp J 6:155–161. https://doi.org/10.1108/13552540010337029

[60] Laumer T, Stichel T, Nagulin K, Schmidt M (2016) Optical analysis of polymer powder materials for Selective Laser Sintering. Polym Test 56:207–213. https://doi.org/10.1016/j.polymertesting.2016.10.010